

## Supporting Information

Sub-chronic exposure to ambient ozone induced liver and lung damage: revealed by lung-liver axis

*Linkang Chen<sup>1#</sup>, Yibin Jia<sup>1#</sup>, Hongtian Su<sup>2</sup>, Liuwen Chen<sup>1</sup>, Ping Zhang<sup>1</sup>, Dan Li<sup>1,3\*</sup>, Jianmin Chen<sup>1</sup>*

<sup>1</sup> Shanghai Key Laboratory of Atmospheric Particle Pollution and Prevention (LAP3), IRDR ICoE on Risk Interconnectivity and Governance on Weather/Climate Extremes Impact and Public Health, Fudan Tyndall Centre, Department of Environmental Science and Engineering, Fudan University, Shanghai 200433, China

<sup>2</sup> Taishan City Center for Disease Control and Prevention, Jiangmen, Guangdong 318000, China

<sup>3</sup> Shanghai Institute of Pollution Control and Ecological Security, Shanghai 200092, China

# Linkang Chen and Yibin Jia are co-first authors.

\* Corresponding authors: Professor Dan Li, Email: [lidanfudan@fudan.edu.cn](mailto:lidanfudan@fudan.edu.cn)

Number of pages 18

Number of texts 2

Number of figures 8

Number of tables 2

## LISTS

**Text S1.** The 16S rRNA gene sequencing and analysis of lung microbiome.

**Text S2.** Measurement of lipidomics in liver

**Fig.S1.** The O<sub>3</sub> exposure system of the study.

**Fig. S2.** Differential lung bacteria in genera levels of different exposure groups.

**Fig. S3.** The Lung Microbiome Health Index and Microbiome Dysbiosis Index analysis.

**Fig. S4.** Levels of oxidative stress indicators in lung tissues of different groups.

**Fig. S5.** Food consumption throughout the animal experiment.

**Fig. S6.** Levels of ALT, AST, TG and GSH in plasma of different groups.

**Fig. S7.** Spearman' s correlation analyses between Fe<sup>2+</sup> with ALT, AST, MDA, GSH and TG of all groups

**Fig. S8.** The relative expression levels of 9 functional genes in the liver (n = 8).

**Table S1.** Nucleotide Sequences of the qPCR Primers.

**Table S2.** Differential comparison of lung microbial community structure.

## **SUPPORTING TEXT**

### **Text S1. The 16S rRNA gene sequencing and analysis of lung microbiome**

#### **DNA extraction, PCR, and Illumina Nextseq 2000 sequencing**

Genomic DNA from individual lung samples were extracted using the NEBNext Microbiome DNA Enrichment Kit (Omega Bio-tek, Norcross, GA, U.S.) according to the manufacturer's instructions. The quality and concentration of DNA were determined by 1.0% agarose gel electrophoresis and a NanoDrop2000 spectrophotometer (Thermo Scientific, United States) and kept at -80 °C prior to further use. The hypervariable region V3-V4 of the bacterial 16S rRNA gene were amplified with primer pairs 338F (5'-ACTCCTACGGGAGGCAGCAG-3') and 806R(5'-GGACTACHVGGGTWTCTAAT-3')<sup>[1]</sup> by T100 Thermal Cycler PCR thermocycler (BIO-RAD, USA). The PCR reaction mixture including 4 µL 5 × Fast Pfu buffer, 2 µL 2.5 mM dNTPs, 0.8 µL each primer (5 µM), 0.4 µL Fast Pfu polymerase, 10 ng of template DNA, and ddH<sub>2</sub>O to a final volume of 20 µL. PCR amplification cycling conditions were as follows: initial denaturation at 95 °C for 3 min, followed by 27 cycles of denaturing at 95 °C for 30 s, annealing at 55 °C for 30 s, and extension at 72 °C for 45 s, and single extension at 72 °C for 10 min, and end at 4 °C. The PCR product was extracted from 2% agarose gel and purified using the PCR Clean-Up Kit (YuHua, Shanghai, China) according to the manufacturer's instructions and quantified using Qubit 4.0 (Thermo Fisher Scientific, USA).

#### **Illumina PE300/PE250 sequencing**

Purified amplicons were pooled in equimolar amounts and paired-end sequenced on an Illumina PE300 platform (Illumina, San Diego, USA) according to the standard protocols by Majorbio Bio-Pharm Technology Co. Ltd. (Shanghai, China). The raw sequencing reads were deposited into the NCBI Sequence Read Archive (SRA) database.

#### **Sequence data analysis**

Quality filtering on the paired-end raw reads were performed under specific filtering conditions to obtain the high-quality clean reads according to the

Trimmomatic (V0.33, <http://www.usadellab.org/cms/?page=trimmomatic>) quality controlled process. Paired-end clean reads were merged using FLASH (V1.2.11, <https://ccb.jhu.edu/software/FLASH/>) according to the relationship of the overlap between the paired-end reads, when at least 10 of the reads overlap the read generated from the opposite end of the same DNA fragment, the maximum allowable error ratio of the overlap region of 0.1, and the spliced sequences were called Raw Tags. Quality filtering, length trimming, and homopolymer truncation were processed using Mothur software (V1.35.1, <http://www.mothur.org>). Sequence analysis was performed by usearch software (V10, <http://www.drive5.com/usearch/>). Sequences with  $\geq 97\%$  similarity were assigned to the same operational taxonomic unit (OTU). The most frequently occurring sequence was extracted as the representative sequence for each OTU and was screened for further annotation using Silva (for 16S, <https://www.arb-silva.de/>) and Unite (for ITS, <http://unite.ut.ee/index.php>) databases with the confidence threshold set to default to  $\geq 0.5$ . The OTU taxonomy synthesis information table (out\_table) for the final analysis was obtained after removing the OTUs and tags, which are annotated as chloroplasts or mitochondria (16S amplicons), or organisms other than fungi (ITS amplicons), and could not be annotated to the kingdom level.

### **Statistical analysis**

Alpha diversity was calculated using QIIME2-2021.2. R software (version R-4.0.2) was used to conduct nonparametric tests on the Alpha diversity index with EasyStat package (wilcoxon. test,  $P < 0.05$  indicates a significant difference). Different letter marks indicate significant differences. Beta diversity was calculated by QIIME2-2021.2. Principal coordinate analysis (PCoA) and visualization were conducted by ggplot2 package based on abund\_jaccard distance. Non-parametric multivariate statistical tests were performed by R(4.0.2) based on vegan package: multivariate analysis of variance based on Bray\_Curtis distance (Analysis of variance, ADONIS), variation analysis between groups (Analysis of similarities, ANOSIM), multiple response permutation procedure (MRPP ). Different species detection between groups: one-way ANOVA test analysis was used to find the biomarker

between groups.

### **Lung Microbiome Health Index (LMHI)**

The Lung Microbiome Health Index (LMHI), a robust index that assesses health status (i.e., the presence of diagnosed disease) based on species-level taxonomic characteristics of lung microbiome samples, focusing on determining the likelihood of disease, independent of clinical diagnosis; This is done by comparing the relative abundance of two groups of microbial species that are associated with good and poor health<sup>1</sup>.

### **Microbiome Dysbiosis Index (MDI)**

The Microbiome Dysbiosis Index (MDI) is an index that determines the degree of microbial imbalance. The higher the value, the greater the degree of bacterial disturbance<sup>2</sup>.

## **Text S2. The 16S rRNA gene sequencing and analysis of lung microbiome**

For the sample preparation ( $n = 6$ ), methods were conducted by a previous study<sup>3</sup>. Briefly, a liver sample (100 mg) was homogenized in 225  $\mu\text{L}$   $-20^{\circ}\text{C}$  methanol containing L-methionine-methyl- $\text{d}_3$  internal standard using a GenoGrinder 2010 (SPEX SamplePrep) at 1,350 rpm for 3 min, followed by sequential addition of 750  $\mu\text{L}$  MTBE (with internal standards), vortexing (30 s),  $4^{\circ}\text{C}$  agitation (5 min), and 188  $\mu\text{L}$  water to induce phase separation after additional vortexing (30 s). After centrifugation (14,000 g, 2 min), 350  $\mu\text{L}$  upper (non-polar) and 250  $\mu\text{L}$  lower (polar) phases were collected and dried, with remaining fractions pooled as Quality control (QC) samples that were injected after every 5 biological samples.

The raw mass spectrometry data were processed through a comprehensive preprocessing pipeline involving peak detection, retention time alignment, and intensity quantification, from which key metabolite features including retention times, compound identities, and peak areas were extracted before being imported into R software (version 4.4.1) for subsequent statistical analysis, with data normalization conducted using internal standards to account for systematic variations, while QC samples were utilized for signal drift correction through the robust spline correction (RSC) algorithm, followed by missing value imputation using the Random Forest method to maintain data integrity and  $\log_2$  transformation to achieve variance stabilization and approximate normality, ultimately enabling the identification of differentially expressed metabolites between experimental groups via orthogonal partial least squares-discriminant analysis (OPLS-DA) with stringent selection criteria of variable importance in projection (VIP) scores  $>1$  and statistically significant P-values  $<0.05$  from Student's t-test.

**SUPPORTING FIGURE**

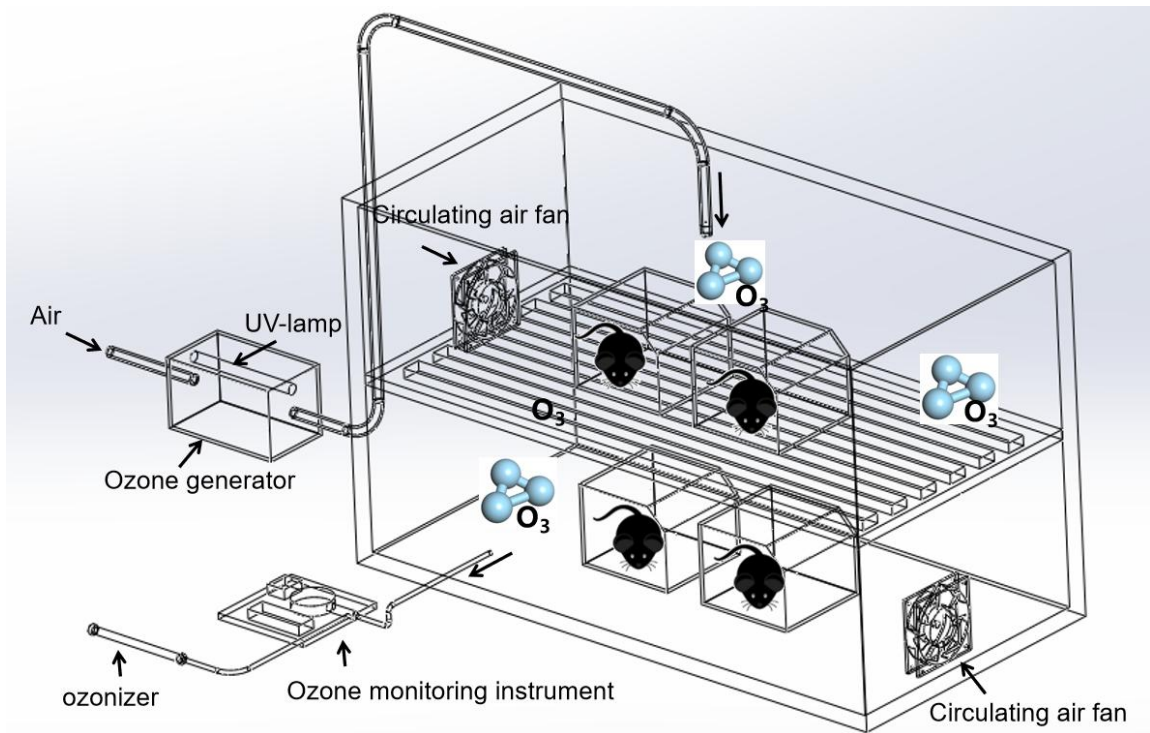


**Fig. S1. The O<sub>3</sub> exposure system of the study.**

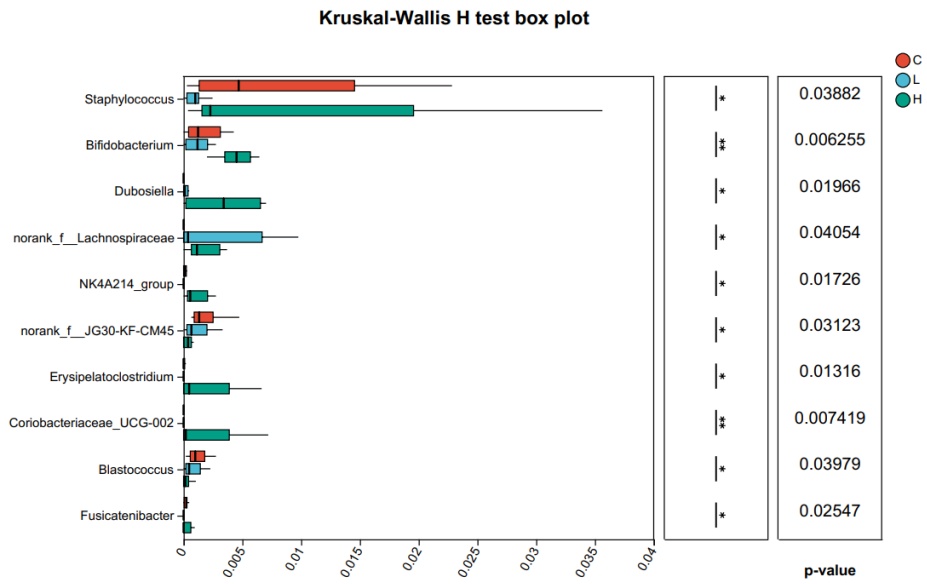


**Fig. S2. Differential lung bacteria in genera level of different exposure groups.**

(\* $p < 0.05$ , \*\* $p < 0.01$ , \*\*\* $p < 0.001$ , \*\*\*\* $p < 0.0001$ ; multiple group comparisons were performed using Kruskal-Wallis test. The C, L, and H represent the control group, low ( $320 \mu\text{g}/\text{m}^3$ ) and high ( $1280 \mu\text{g}/\text{m}^3$ ) groups, respectively.

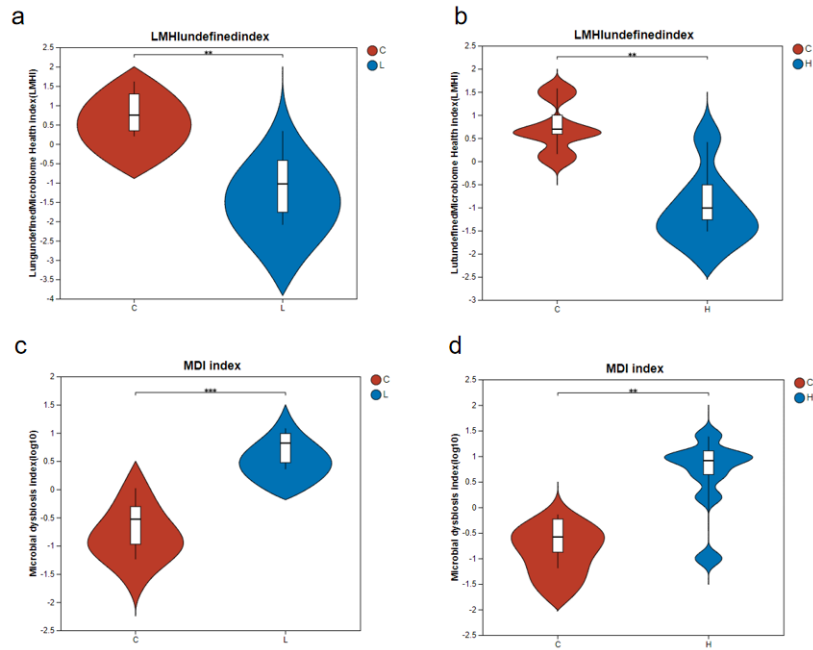


**Fig. S3. The Lung Microbiome Health Index and Microbiome Dysbiosis Index analysis. (a-b)** represents the LMHI index in the fecal of different groups. **(c-d)** represents MDI index in lung of different groups. The C, L, and H represent the control group, mice exposed to low ( $320 \mu\text{g}/\text{m}^3$ ) and high ( $1280 \mu\text{g}/\text{m}^3$ ) concentrations of ozone groups respectively. Difference group comparisons were performed using the student *t-test*,  $*P < 0.05$ .

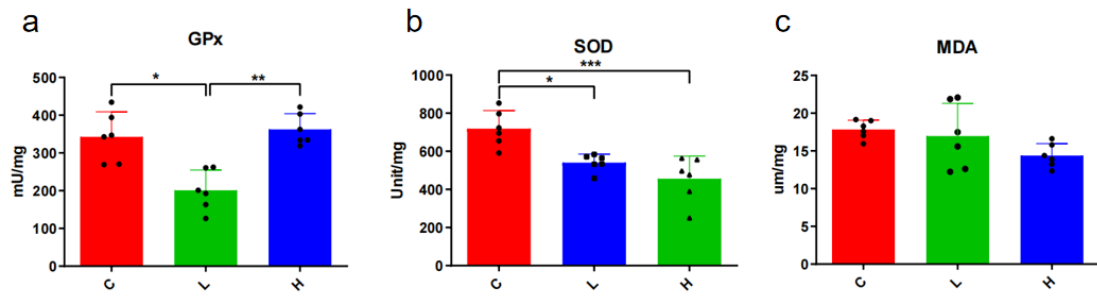


**Fig. S4. Levels of oxidative stress indicators in lung tissues of different groups ( $n = 6$ ).** The C, L, and H represent the control group, mice exposed to low ( $320 \mu\text{g}/\text{m}^3$ ) and high ( $1280 \mu\text{g}/\text{m}^3$ ) concentrations of ozone groups respectively. multiple group comparisons were performed using a one-way ANOVA test. \* $p < 0.05$ , \*\* $p < 0.01$ , \*\*\* $p < 0.001$

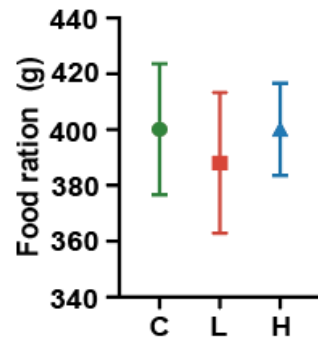


**Fig. S5. Food consumption throughout the animal experiment.** The C, L, and H represent the control group, mice exposed to low ( $320 \mu\text{g}/\text{m}^3$ ) and high ( $1280 \mu\text{g}/\text{m}^3$ ) concentrations of ozone groups respectively.

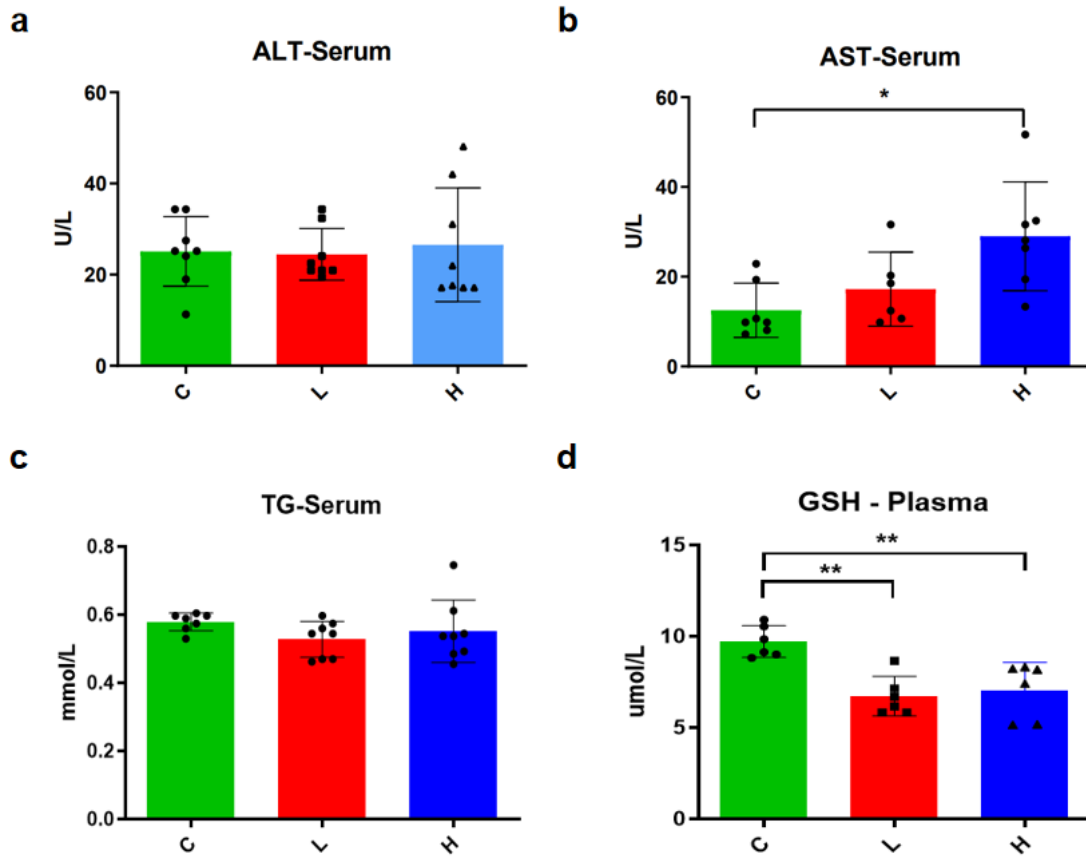


**Fig. S6. Levels of liver functional in serun and GSH in plasma of different groups ( $n = 6-8$ ).** The C, L, and H represent the control group, mice exposed to low ( $320 \mu\text{g}/\text{m}^3$ ) and high ( $1280 \mu\text{g}/\text{m}^3$ ) concentrations of ozone groups respectively. multiple group comparisons were performed using a one-way ANOVA test. \* $p < 0.05$ , \*\* $p < 0.01$ , \*\*\* $p < 0.001$ .

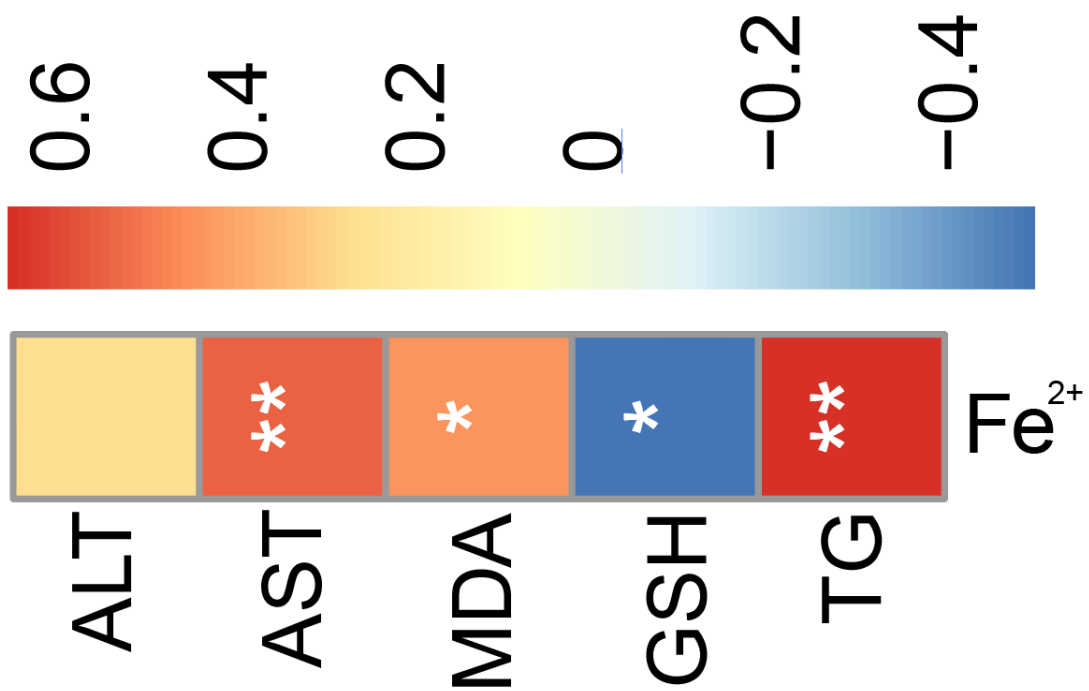


**Fig. S7.** Spearman's correlation analyses between  $\text{Fe}^{2+}$  with ALT, AST, MDA, GSH and TG of all groups. \* $p < 0.05$ , \*\* $p < 0.01$ .

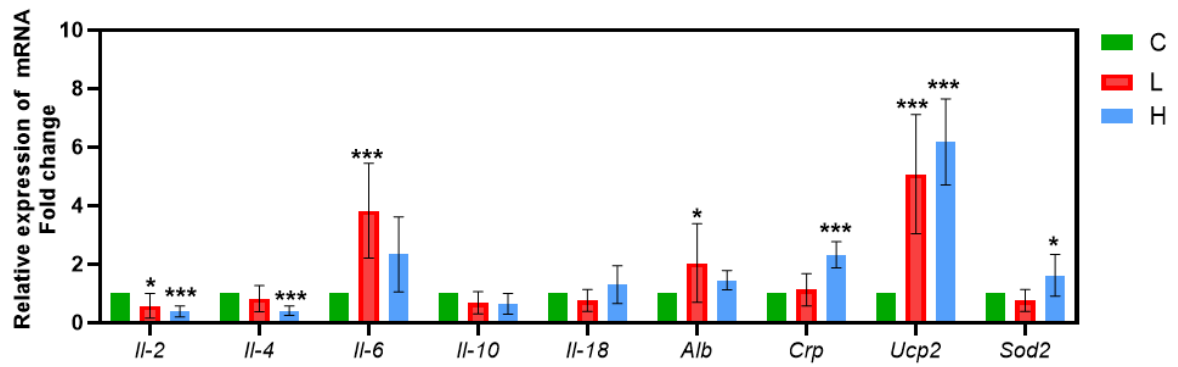


**Fig. S8. The relative expression levels of 9 functional genes in the liver ( $n = 6-8$ ).**

The C, L, and H represent the control group, mice exposed to low ( $320 \mu\text{g}/\text{m}^3$ ) and high ( $1280 \mu\text{g}/\text{m}^3$ ) concentrations of ozone groups respectively. multiple group comparisons were performed using a one-way ANOVA test. \* $p < 0.05$ , \*\* $p < 0.01$ , \*\*\* $p < 0.001$ .

## SUPPORTING TABLE

**Table S1. Nucleotide Sequences of the qPCR Primers.**

Gene	Sequence (5'→3')
<i>Gapdh</i>	AGGTCGGTGTGAACGGATTTG
	GGGGTCGTTGATGGCAACA
<i>Occludin</i>	TGAACAGCCCCCAATGT
	TCAACTCTTTCCGCATAGTCAGAT
<i>Zo-1</i>	GCTTTAGCGAACAGAAGGAGC
	TTCATTTTTCCGAGACTTCACCA
<i>Hmox-1</i>	AGGGCTCGGAACTCCAGAAA
	CCAGGGAATCGGTAGACATCG
<i>Sod2</i>	GTTACAACCTCAGGTCGCTCTTCAG
	TGATAGCCTCCAGCAACTCTCC
<i>Ucp2</i>	GCTGGTGGTGGTCGGAGATAC
	GCACAGTTGACAATGGCATTACG
<i>Nfe2l2</i>	AAGCACAGCCAGCACATTCTC
	ACCAGGACTCACGGGAACTTC
<i>Nos3</i>	GCCTAGTCCTCGCCTCCTTC
	TGAACCACTTCCATTCTTCGTAGC
<i>Cat</i>	CGTCCGTCCTGCTGTCTC
	GCTCCTTCCACTGCTTCATCTG
<i>Gstp1</i>	GCTGGAAGGAGGAGGTGGTTAC
	AGGTGTCTCAAGATGGCATTAGATTG
<i>Il-1β</i>	TCGCTCAGGGTCACAAGAAA
	CATCAGAGGCAAGGAGGAAAAC
<i>Il-2</i>	TGAGCAGGATGGAGAATTACAGG
	GTCCAAGTTCATCTTCTAGGCAC
<i>Il-4</i>	GGTCTCAACCCCCAGCTAGT

	GCCGATGATCTCTCTCAAGTGAT
--	-------------------------

Gene	Sequence (5'->3')
<i>Il-6</i>	CTGCAAGAGACTTCCATCCAGTT
	GAAGTAGGGAAGGCCGTGG
<i>Il-10</i>	GCTCTTACTGACTGGCATGAG
	CGCAGCTCTAGGAGCATGTG
<i>Il-18</i>	GACTCTTGCGTCAACTTCAAGG
	CAGGCTGTCTTTTGTCAACGA
<i>Tlr-4</i>	GCCTTTCAGGGAATTAAGCTCC
	GATCAACCGATGGACGTGTAAA
<i>Mmp9</i>	GCTGACTACGATAAGGACGGCA
	TAGTGGTGCAGGCAGAGTAGGA
<i>Crp</i>	TTCCAAGGAGTCAGATACTTCC
	TCAGAGCAGTGTAGAAATGGAGA
<i>Alb</i>	GACGTGTGTTGCCGATGAGT
	GTTTTACGGAGGTTTGAATG

**Table S2. Differential comparison of lung microbial community structure.**

Adonis	Df	Sums_of_sqs	F.Model	R <sup>2</sup>	Pr (>F)
Group factors	2	0.7995	1.6751	0.1376	0.05
Residuals	21	5.0115	-	0.8624	0
Total	23	5.811	-	1	0

**Note:** The C, L, and H represent the control group, mice exposed to low (320 µg/m<sup>3</sup>) and high (1280 µg/m<sup>3</sup>) concentrations of ozone groups respectively.

**Adonis:** F represents F test value, and R<sup>2</sup> represents the interpretation degree of sample difference by different groups. The larger F and R<sup>2</sup> are, the higher the degree of group difference is.  $P < 0.05$  indicates that the test has a high feasibility.

## REFERENCES

1. Gupta, V. K. *et al.* A predictive index for health status using species-level gut microbiome profiling. *Nat. Commun.* **11**, 4635 (2020).
2. Gunathilake, M. *et al.* Alterations in Gastric Microbial Communities Are Associated with Risk of Gastric Cancer in a Korean Population: A Case-Control Study. *Cancers* **12**, 2619 (2020).
3. Huang, Z., L.*et al.* Long-term chronic food-derived arsenic exposure induce the urinary system metabolic dysfunction in mice. *Sci Total Environ.* 2023